Catalysis Today 146 (2009) 141–147

Contents lists available at ScienceDirect

Catalysis Today

journal homepage: www.elsevier.com/locate/cattod

Catalytic properties and coking stability of new anode materials for internal methane reforming in the intermediate temperature solid oxide fuel cells

Tamara Kharlamova [a,*], Svetlana Pavlova [a], Vladislav Sadykov [a], Tamara Krieger [a], Galina Alikina [a], Christos Argirusis [b]

[a] Boreskov Institute of Catalysis, Pr. Lavrentieva, 5, 630090, Novosibirsk, Russia
[b] Clausthal University of Technology, 38678, Clausthal-Zellerfeld, Germany

ARTICLE INFO

Article history:
Available online 18 March 2009

Keywords:
Anode
Internal methane reforming
Coking stability
IT SOFC
Apatite-type lanthanum silicates

ABSTRACT

Catalytic properties and coking stability of composite materials based on NiO and doped apatite-type lanthanum silicates were studied for their using as anode materials for internal methane reforming in intermediate temperature solid oxide fuel cells. Samples based on Sr- or Al-doped lanthanum silicate were prepared by modified Pechini methods. The composite materials were characterized by X-ray diffraction, methane steam reforming and temperature programmed oxidation. The effects of $La_{0.8}Sr_{0.2}Mn_{0.8}Cr_{0.2}O_3$ addition, partial Ni substitution with $La_{0.1}Sr_{0.9}TiO_3$ ionic and electronic mixed conductor and composition of apatite-type lanthanum silicate on catalytic properties and coking resistance were considered.

1. Introduction

Solid oxide fuel cells (SOFCs), possessing a high efficiency of energy conversion, attract a great attention among other types of fuel cells due to simplicity of system design, relatively low sensitivity to impurities in the fuel, multi-fuel capability and possibility of direct hydrocarbon oxidation without external reforming [1–3]. The reduction of the cell operation temperatures below 800 °C can make this technology more commercially attractive and expand a field of SOFC application [1]. The development of advanced materials is one of the aspects in design of intermediate temperature (IT) SOFC.

Recently, apatite-type lanthanum silicates (ATLS) were shown to be promising electrolyte materials possessing a higher conductivity at IT in comparison with well-known yttria-stabilized zirconia (YSZ) [4,5]. Using new electrolytes, in turn, necessitates the development of novel anode materials to provide compatibility of SOFC components and feasibility of the direct fuel conversion using both hydrogen and hydrocarbons. Unfortunately, in spite of ATLS to be considered as promising electrolyte materials for IT SOFCs, nowadays only scarce studies devoted to the development of suitable electrodes for new electrolytes are presented in the literature [6–11]. Thus, there are few papers which report performance of fuel cells using lanthanum silicate-based electrolytes and Pt electrodes [6–8]. More recently, Yoshioka et al. reported that using cermets anode, $Ni/Sm_{0.2}Ce_{0.8}O_{1.9}$ and ceramic cathode, $La_{0.9}Sr_{0.1}CoO_{3-\delta}$ instead of Pt electrodes results in cell performance improvement [9]. Another cermets to be considered as a fuel electrode for ATLS-based SOFCs are Ni/apatite, in particularly $Ni/La_9SrSi_6O_{26.5}$ [10,11].

The composite anodes consisting of metal-oxide cermets (Ni/YSZ, $Ni/Ce_{1-x}Gd_xO_{2-\delta}$, Ni–Co/YSZ, Ni–Cu/YSZ, Cu/YSZ, etc.) have been mainly accepted, Ni-based cermets remaining the most suitable due to their high catalytic and electrochemical activity along with a low cost [12,13]. On the other hand, using Ni-based cermets anode for direct hydrocarbons conversion can be complicated by strong coking resulting in anode degradation [12]. However, the possibility of direct using methane and other hydrocarbons makes SOFCs so promising as electric power stations. Thus, study of the catalytic activity and the carbon resistance of anode materials is important task for the anode development.

This manuscript is devoted to the study of the catalytic activity and coking stability of Ni/apatite based cermets in methane steam reforming [14]. To prevent strong coking of composites the sample promotion by $La_{0.8}Sr_{0.2}Mn_{0.8}Cr_{0.2}O_3$ oxide possessing a high mobility of the lattice oxygen and/or partial substitution of Ni for $La_{0.1}Sr_{0.9}TiO_3$ oxide having high mixed ionic and electronic conductivity were used [12].

* Corresponding author. Tel.: +7 383 3307672; fax: +7 383 3309687.
E-mail address: kharlamova@catalysis.ru (T. Kharlamova).

0920-5861/$ – see front matter © 2009 Elsevier B.V. All rights reserved.
doi:10.1016/j.cattod.2009.01.052

2. Experimental

Composite materials comprised of $(30 - x)$ wt.% Ni – x wt.% LST – y wt.% LSMC–ATLS ($x = 0$, 5, 10 or 20; $y = 0$ or 10) were prepared using modified Pechini (Pe) method. For this, powders of Sr- or Al-doped ATLS and $La_{0.1}Sr_{0.9}TiO_3$ (LST) were added to a gel of organometallic precursors of NiO or NiO–$La_{0.8}Sr_{0.2}Mn_{0.8}Cr_{0.2}O_3$ (LSMC) followed by stirring at 80 °C for 1 h for a system homogenization. The procedure of the gel preparation is described in details elsewhere [15]. The mixture obtained was calcined at 50–600 °C for pyrolysis of polymer precursors, reground and finally calcined at 700 °C.

The samples were characterized by X-ray diffraction (XRD), BET specific surface area (SSA) and catalytic testing. XRD patterns were recorded with URD-6M or ARL'TRA θ–θ diffractometers using Cu Kα radiation. The SSA of samples was measured by Ar thermal desorption.

The catalytic activity in methane SR was tested in a plug-flow reactor at 600–800 °C using a stepwise heating at 700 °C for about 5 h or until the sample deactivation. The flow of 7% CH_4–7% H_2O in He (10 L h^{-1}) was used as a feed. About 0.15–0.24 g of the sample (0.25–0.5 mm; 0.14 cm^3) diluted by quartz (0.5–1 mm; 2 cm^3) were typically used for the catalytic testing. The contact time was 50 ms. Prior to the experiment sample was reduced with the flow of 20% H_2 in He for 0.5 h at 700 °C.

The conversions of CH_4 (X_{CH4}) and product selectivity (S_i, $i = CO_2$, CO, H_2) are defined as

$$X_{CH_4}\ (\%) = \frac{[C_{CH_4}(\text{in}) - C_{CH_4}(\text{out})]}{C_{CH_4}(\text{in})} \times 100, \quad (1)$$

$$S_{CO_2}\ (\%) = \frac{C_{CO_2}(\text{out})}{[C_{CH_4}(\text{in}) - C_{CH_4}(\text{out})]} \times 100, \quad (2)$$

$$S_{CO}\ (\%) = \frac{C_{CO}(\text{out})}{[C_{CH_4}(\text{in}) - C_{CH_4}(\text{out})]} \times 100, \quad (3)$$

$$S_{H_2}\ (\%) = \frac{C_{H_2}(\text{out})}{3 \times [C_{CH_4}(\text{in}) - C_{CH_4}(\text{out})]} \times 100, \quad (4)$$

where C(in) and C(out) are concentration (vol.%) before and after the reaction, respectively. All concentrations were used with a glance of a flow dilution.

The expression (4) supposes the H_2 formation only according to the reaction (5)

$$CH_4 + H_2O \rightarrow CO + 3H_2. \quad (5)$$

The H_2 formation due to methane decomposition (6)

$$CH_4 \rightarrow C + 2H_2 \quad (6)$$

or water-shift reaction (7)

$$CO + H_2O \rightarrow CO_2 + H_2 \quad (7)$$

was not discounted. This can result in observed H_2 selectivity to be higher then C-product selectivity.

Samples after testing were studied by temperature programmed oxidation (TPO) in the temperature range of 25–880 °C. This was carried out in the flow kinetic installations using about 0.02 g of the sample diluted by quartz (0.5–1 mm; 0.1 cm^3), 1% O_2 in He (10 L h^{-1}) and heating rate of 5 °C/min.

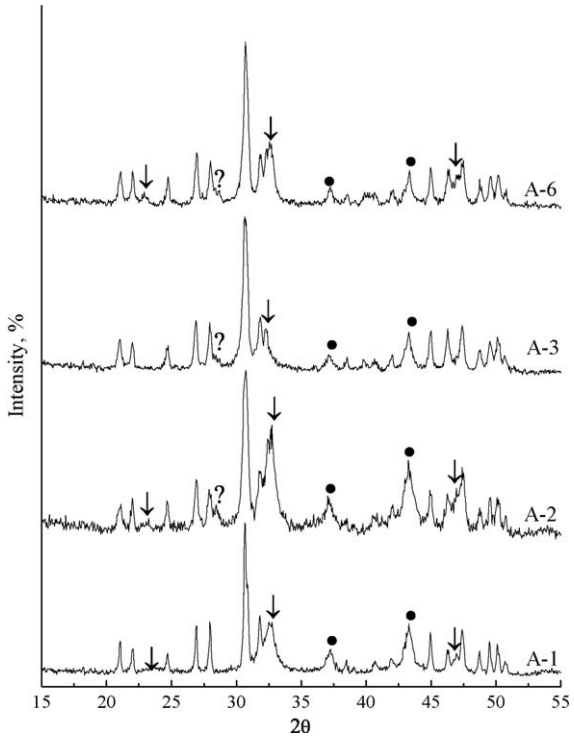

Fig. 1. Typical X-ray diffraction patterns of anode composites based on Mg- and Sr-doped apatite-type lanthanum silicates: (●) NiO, (↓) perovskite, (?) not reliably identified phase, (unmarked reflections) apatite: A-1, 30 wt.% Ni/70 wt.% $La_9Mg_{0.5}Si_6O_{26}$; A-2, 30 wt.% Ni/10 wt.% $La_{0.8}Sr_{0.2}Mn_{0.8}Cr_{0.2}O_3$/60 wt.% $La_9SrSi_6O_{26.5}$; A-3, 15 wt.% Ni/15 wt.% $La_{0.1}Sr_{0.9}TiO_3$/60 wt.% $La_9SrSi_6O_{26.5}$; A-6, 15 wt.% Ni/15 wt.% $La_{0.1}Sr_{0.9}TiO_3$/10 wt.% $La_{0.8}Sr_{0.2}Mn_{0.8}Cr_{0.2}O_3$/60 wt.% $La_9SrSi_6O_{26.5}$.

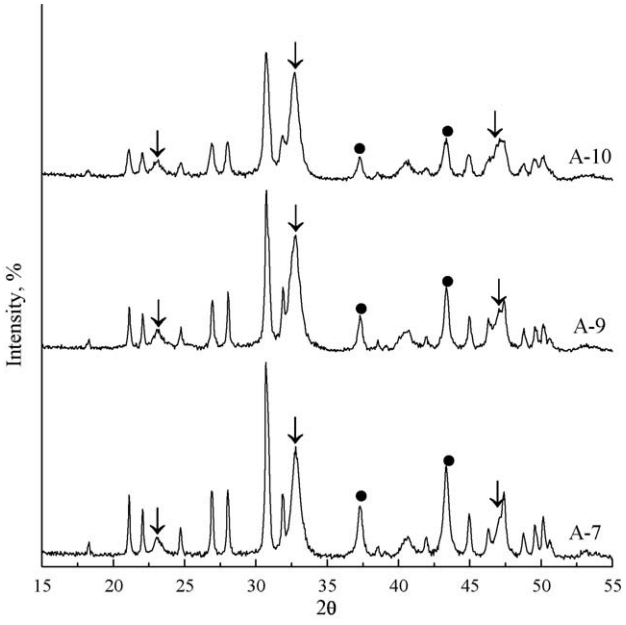

Fig. 2. Typical X-ray diffraction patterns of anode composites based on Al-doped apatite-type lanthanum silicates: (●) NiO, (↓) perovskite, (unmarked reflections) apatite: A-7, 30 wt.% Ni/10 wt.% $La_{0.8}Sr_{0.2}Mn_{0.8}Cr_{0.2}O_3$/60 wt.% $La_{9.83}Si_5AlO_{26.25}$; A-9, 20 wt.% Ni/10 wt.% $La_{0.1}Sr_{0.9}TiO_3$/10 wt.% $La_{0.8}Sr_{0.2}Mn_{0.8}Cr_{0.2}O_3$/60 wt.% $La_{9.83}Si_5AlO_{26.25}$; A-10, 15 wt.% Ni/15 wt.% $La_{0.1}Sr_{0.9}TiO_3$/10 wt.% $La_{0.8}Sr_{0.2}Mn_{0.8}Cr_{0.2}O_3$/60 wt.% $La_{9.83}Si_5AlO_{26.25}$.

Table 1
Composition and some structural characteristics of prepared anode composites: LSMC, $La_{0.8}Sr_{0.2}Mn_{0.8}Cr_{0.2}O_3$; LST, $La_{0.1}Sr_{0.9}TiO_3$; L7SSi, $La_7Sr_3Si_6O_{25.5}$; LMSi, $La_9Mg_{0.5}Si_6O_{26}$; L9SSi, $La_9SrSi_6O_{26.5}$; LSiA, $La_{9.83}Si_5AlO_{26.25}$; SSA, specific surface area; d_{XRD}, mean crystallite size of NiO according X-ray diffraction data.

Sample	Ni (wt.%)	LST (wt.%)	LSMC (wt.%)	Electrolite	SSA (m^2/g)	d_{XRD} (nm)
A-1	30	–	–	LMSi	42	13
A-2	30	–	10	L9SSi	29	10
A-3	15	15	–	L9SSi	17	10
A-4	25	5	10	L9SSi	22	24
A-5	20	10	10	L9SSi	31	25
A-6	15	15	10	L9SSi	16	14
A-7	30	–	10	LSiA	22	21
A-8	25	5	10	LSiA	21	21
A-9	20	10	10	LSiA	21	24
A-10	15	15	10	LSiA	18	20

3. Results and discussion

3.1. Sample characterization

The compositions and some structural characteristics of synthesized anode materials are presented in Table 1. Following to Brisse and Beaudet-Savignat [10,11], the parent composite (A-1) contains NiO (to provide both a high electron conductivity and a catalytic activity of the fuel electrode) and ATLS (electrolyte, in particular, to provide thermal expansion matching of the SOFC component and to inhibit coarsening and grain growth of the Ni phase) [3,12]. To provide the feasibility of the direct methane conversion, the anode composition was modified. For that, the additive of LSMC and/or partial Ni substitution by LST was used (Table 1). Besides, ATLS electrolytes with a different dopant nature were used for composite preparation.

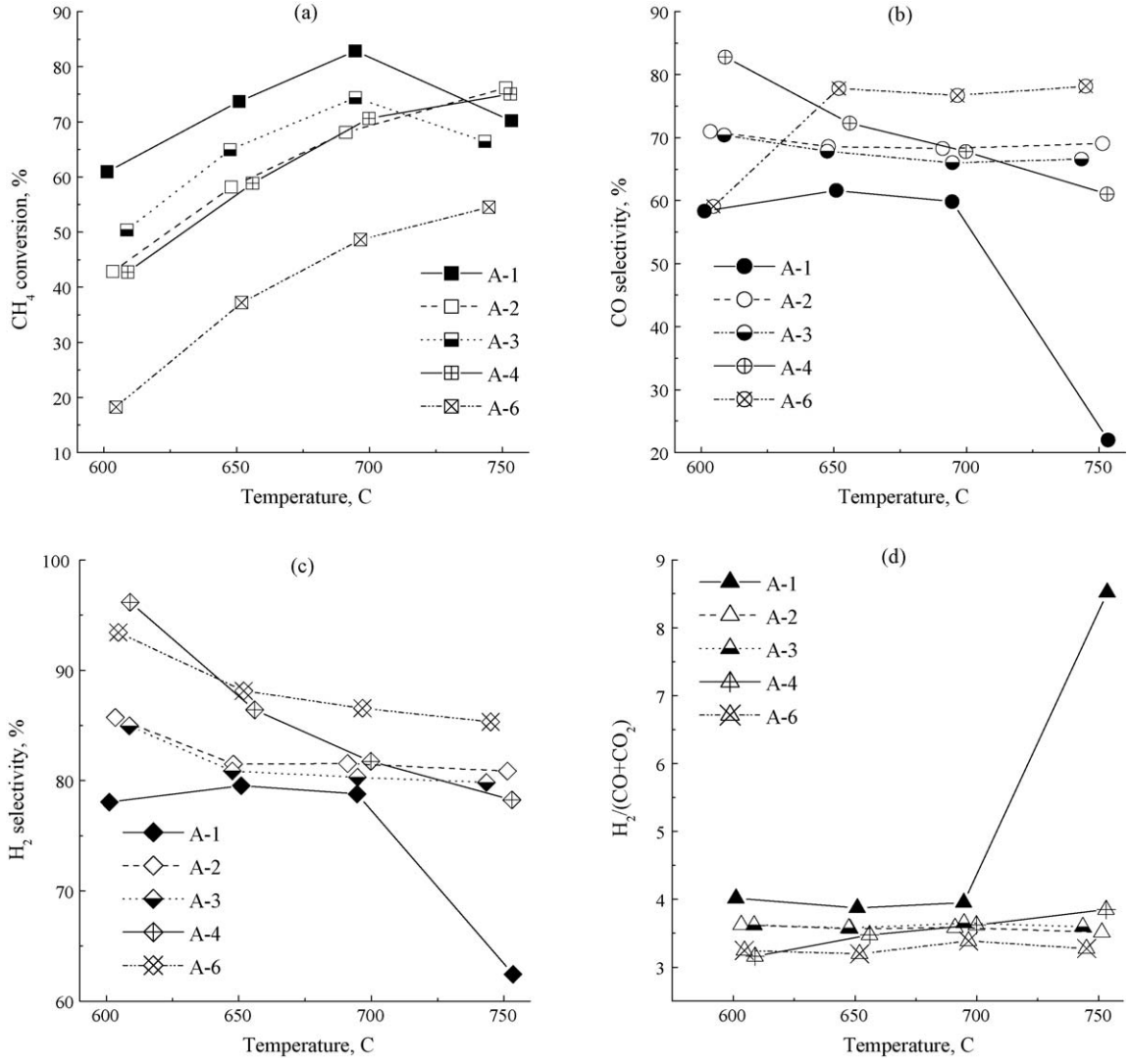

Fig. 3. Temperature dependence of methane conversion (a), CO selectivity (b), H_2 selectivity (c) and $H_2/(CO + CO_2)$ mole ratio in the products (d): A-1, 30 wt.% Ni/70 wt.% $La_9Mg_{0.5}Si_6O_{26}$; A-2, 30 wt.% Ni/10 wt.% $La_{0.8}Sr_{0.2}Mn_{0.8}Cr_{0.2}O_3$/60 wt.% $La_9SrSi_6O_{26.5}$; A-3, 15 wt.% Ni/15 wt.% $La_{0.1}Sr_{0.9}TiO_3$/60 wt.% $La_9SrSi_6O_{26.5}$; A-4, 25 wt.% Ni/5 wt.% $La_{0.1}Sr_{0.9}TiO_3$/10 wt.% $La_{0.8}Sr_{0.2}Mn_{0.8}Cr_{0.2}O_3$/60 wt.% $La_9SrSi_6O_{26.5}$; A-6, 15 wt.% Ni/15 wt.% $La_{0.1}Sr_{0.9}TiO_3$/10 wt.% $La_{0.8}Sr_{0.2}Mn_{0.8}Cr_{0.2}O_3$/60 wt.% $La_9SrSi_6O_{26.5}$. The characteristics presented were obtained using a stepwise heating and correspond to values after 20–30 min in stream at each temperature.

Typical XRD patterns of the samples are shown in Figs. 1 and 2. According to XRD data, all prepared samples contain apatite, perovskite and NiO phases. For the samples A-4, A-5, A-6, A-8, A-9 and A-10 simultaneously containing LST and LSMC, it is not possible to identify the presence of both perovskite-type phases due to overlap and broadening of the reflections. Besides, the real composition of the perovskite observed is also affected by the presence of NiO precursor in the starting gel along with those of LSMC as well as partial dissolution of ATLS and LST under acid conditions during the sample preparation. Thus, reflections of the perovskite-type phase are observed in the pattern of the unpromoted A-1 sample (Fig. 1). These seem to be caused by washing-out of some La from the solid ATLS during the sample preparation due to acid conditions of the gel followed by the formation of the perovskite phase during sample calcination. Note, that in the case of a sample prepared via wetness impregnation, the surface interaction between ATLS and NiO precursor was shown to result in the formation of the tetragonal-type La_2NiO_4 [16].

Element redistribution during multicomponent sample preparation also results in the formation of some phase in anode materials based on Sr-doped ATLS that was not reliably identified (Fig. 1). This phase is not observed in the patterns of samples based on Al-doped ATLS (Fig. 2). Besides, reflections of this phase are observed in the pattern of the A-3 sample that is not promoted by LSMC. This lets to surmise that some SrO_2 (PDF 07-0234) can also be formed during the sample preparation in the materials based on Sr-doped ATLS.

According to XRD data, the mean crystallite size of NiO for all systems does not exceed 25 nm (Table 1). The SSA of the anode materials is higher than 16 m^2/g. The typical SSA of the anode material prepared by the conventional ceramic mixing process is lower 8 m^2/g [12]. Besides, this method of the anode preparation does not provide a good homogeneity of Ni and YSZ phase distribution. The structural/morphological features of samples prepared by Pe method can significantly affect microstructure and electrical conductivity of the fuel electrode [12,17]. In addition, the

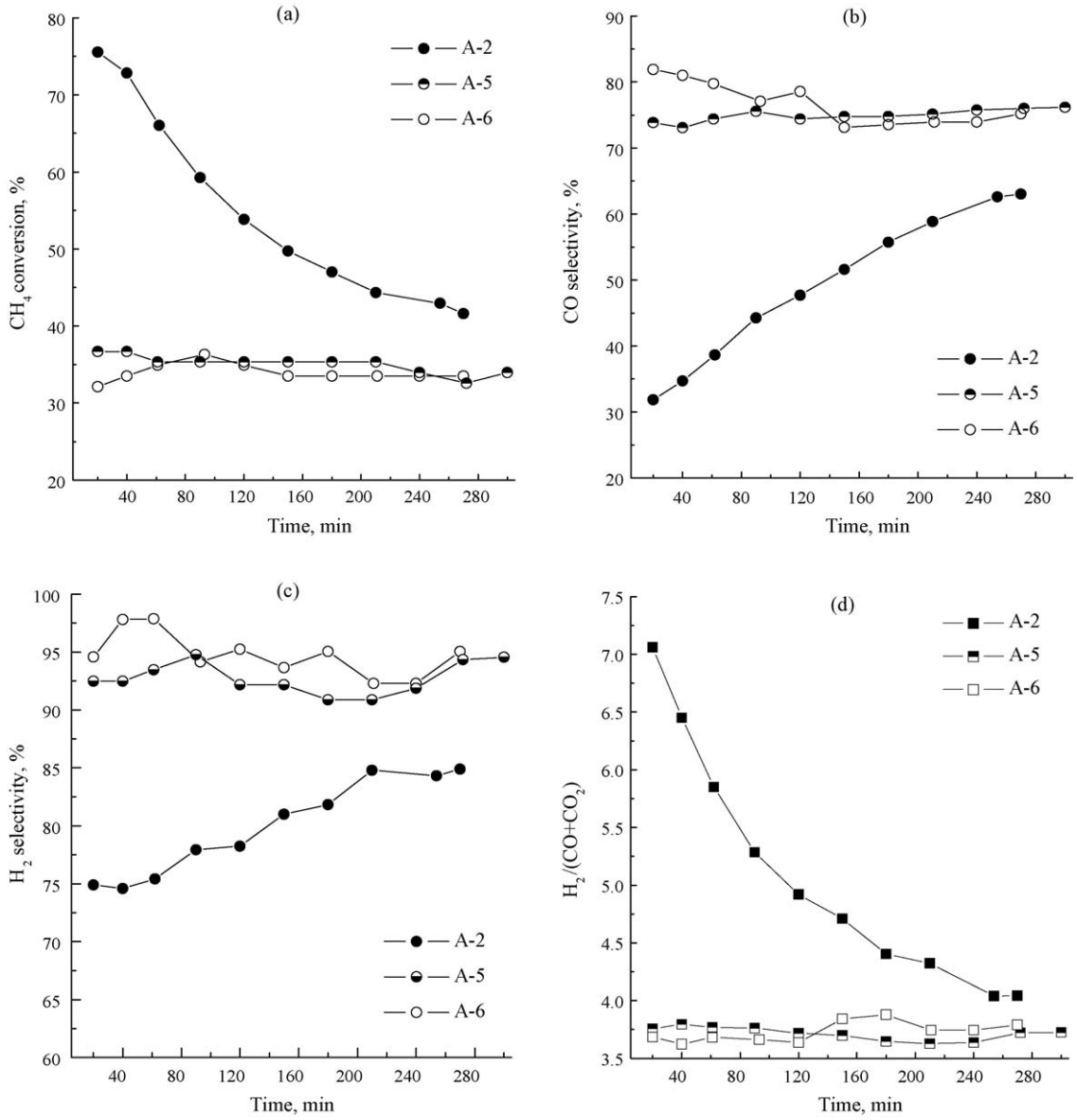

Fig. 4. Time dependence of methane conversion (a), CO selectivity (b), H_2 selectivity (c) and $H_2/(CO + CO_2)$ mole ratio in the products (d) at 700 °C for anode composites based on Sr-doped apatite-type lanthanum silicates: A-2, 30 wt.% Ni/10 wt.% $La_{0.8}Sr_{0.2}Mn_{0.8}Cr_{0.2}O_3$/60 wt.% $La_9SrSi_6O_{26.5}$; A-5, 20 wt.% Ni/10 wt.% $La_{0.1}Sr_{0.9}TiO_3$/10 wt.% $La_{0.8}Sr_{0.2}Mn_{0.8}Cr_{0.2}O_3$/60 wt.% $La_9SrSi_6O_{26.5}$; A-6, 15 wt.% Ni/15 wt.% $La_{0.1}Sr_{0.9}TiO_3$/10 wt.% $La_{0.8}Sr_{0.2}Mn_{0.8}Cr_{0.2}O_3$/60 wt.% $La_9SrSi_6O_{26.5}$.

applied method allowed improving the spatial uniformity of the phase distribution in the anode powders.

3.2. Catalytic activity

3.2.1. The unmodified composite

The unmodified A-1 catalyst shows rather high initial (for 20–30 min) activity in methane steam reforming in the stoichiometric feed at 600–700 °C and the short contact time (Fig. 3a). However, subsequent testing at the higher temperature (Fig. 3a) results in a decline of methane conversion because of the sample deactivation due to coke formation. Indeed, on the contrast to the high conversion, the A-1 sample provides relatively low C-product ($CO + CO_2$) selectivity at all studied temperatures. CO_2 formation (not shown here) is significant (9-2%) only at 600–650 °C. At higher temperatures it was not practically detected. CO selectivity of the A-1 sample does not exceed 62%, being greatly reduced during testing at 700–750 °C (Fig. 3b). Besides, a higher H_2 selectivity in comparison with that of $CO + CO_2$ due to methane decomposition also indicates strong coking of the sample (Fig. 3c and d). This makes the unpromoted sample to be unsuitable for using as an anode material for direct SOFC, in spite of the high methane conversion. To prevent strong coking of Ni-anode materials during SOFC operation, different ways are discussed in literature including addition of oxides with high oxygen mobility and Ni substitution for other metals or mixed ionic and electronic conducting (MIEC) oxides [3,12,18–20].

3.2.2. The effect of the sample modification

Some our results for anode sample modified by LSMC or LST are presented in Fig. 3. According to presented data, using both LSMC [12,14] as an anode promoter and partial Ni substitution by LST MIEC [12,21], favours methane oxidation and prevents carbon formation as compared with the A-1 sample (Fig. 3). Thus, it can be seen that methane conversion of A-2 and A-3 samples is lower and its CO selectivity is higher at 600–750 °C (Fig. 3a and b). Besides, H_2 selectivity, being higher than that of C-product, does not exceed it for more than 20 rel.% for both A-2 and A-3 samples. The H_2/C ratio does not significantly vary during testing at 650–750 °C.

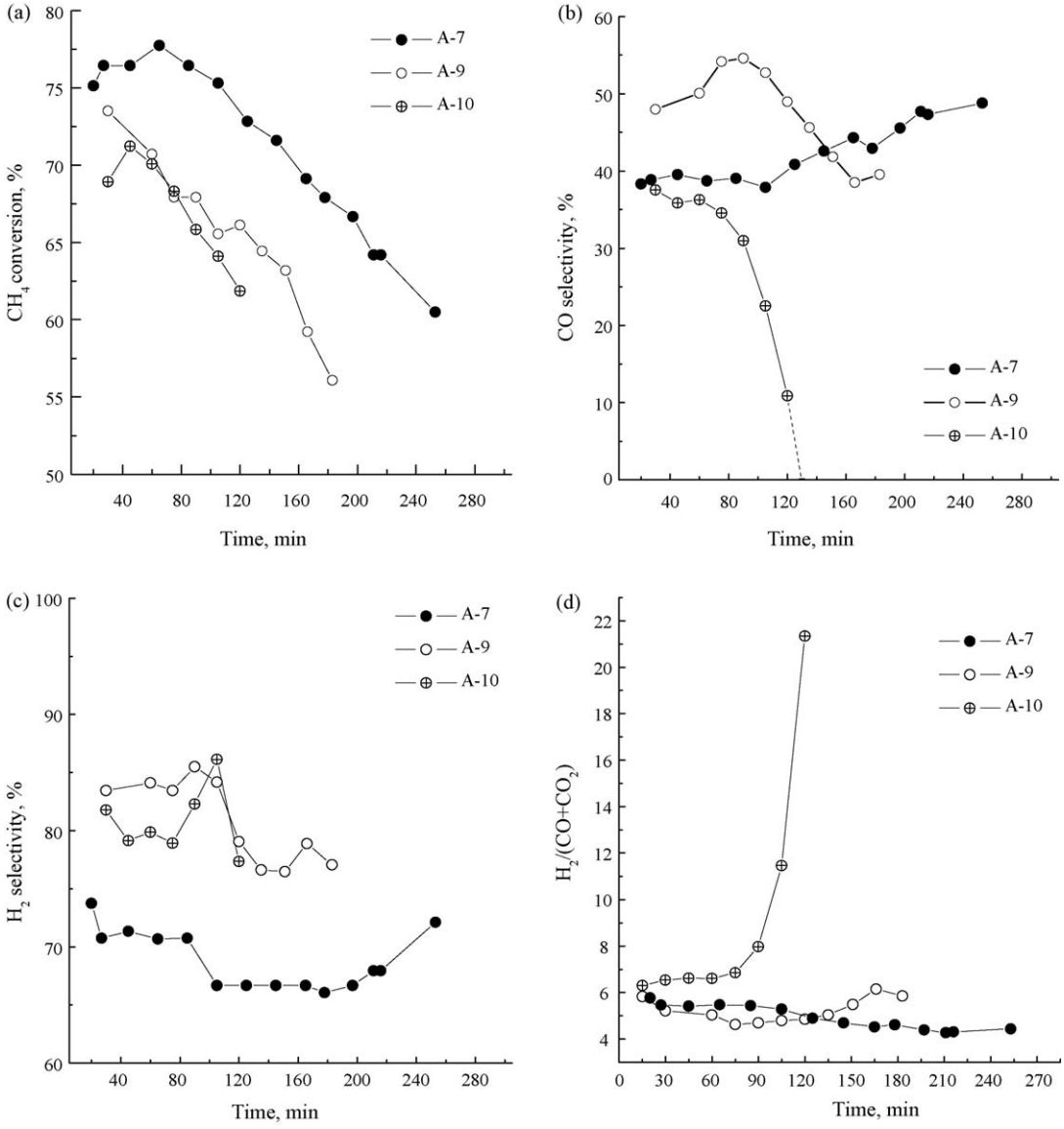

Fig. 5. Time dependence of methane conversion (a), CO selectivity (b), H_2 selectivity (c) and $H_2/(CO + CO_2)$ mole ratio in the products (d) at 700 °C for anode composites based on Al-doped apatite-type lanthanum silicates: A-7, 30 wt.% Ni/10 wt.% $La_{0.8}Sr_{0.2}Mn_{0.8}Cr_{0.2}O_3$/60 wt.% $La_{9.83}Si_5AlO_{26.25}$; A-9, 20 wt.% Ni/10 wt.% $La_{0.1}Sr_{0.9}TiO_3$/10 wt.% $La_{0.8}Sr_{0.2}Mn_{0.8}Cr_{0.2}O_3$/60 wt.% $La_{9.83}Si_5AlO_{26.25}$; A-10, 15 wt.% Ni/15 wt.% $La_{0.1}Sr_{0.9}TiO_3$/10 wt.% $La_{0.8}Sr_{0.2}Mn_{0.8}Cr_{0.2}O_3$/60 wt.% $La_{9.83}Si_5AlO_{26.25}$.

However, for the A-3 catalyst, some methane conversion decrease is observed at 750 °C and prolonged testing at 700 °C show its insufficient stability (Fig. 4). Thus, a high initial methane conversion is accompanied by a high H_2/C ratio due to coke formation. Further testing results in a gradual decrease of the methane conversion. At the same time, CO and H_2 selectivity increases and the H_2/C ratio decreases during the experiment. This suggests that mainly coke formation is suppressed while sites, which are active in methane oxidation, are not practically deactivated. The latter appear to be favoured by LSMC addition. For further improving the catalytic characteristics and suppression of the coke formation, the partial Ni substitution by LST for samples promoted by LSMC was used.

3.2.3. The effect of simultaneous LSMC addition and partial Ni substitution

The replacement of 5% Ni by LST (the sample A-4) does not essentially improve the catalytic performance of the composite (Fig. 3). In comparison to the A-2 sample, methane conversion is not practically changed at 600–750 °C. An appreciable increase of the target product selectivity is observed at 600–650 °C. However, it decreases at higher temperatures, especially for C-products. This is accompanied by the decrease of H_2/C ratio with the temperature increase (Fig. 3d).

The substitution of 50% Ni in the A-6 sample results in a significant decrease of the methane conversion in comparison with that of above considered samples (Fig. 3a). At the same time, C-product and H_2 selectivity are considerably higher for the A-6 at all temperatures. The H_2/C ratio, being the lowest, is practically unchanged during the experiment (Fig. 3d). Besides, no significant changes are observed in methane conversion or product selectivity during testing at 700 °C for about 5 h (Fig. 4). A similar result was obtained for the A-5 sample where 33% of Ni was substituted by LST (Fig. 4).

It is to be also noted, that, in spite of the total conversion of methane is strongly decreased for A-5 and A-6 composites, the catalytic activity toward steam reforming at 700 °C – specific reaction rate of CO formation, mL CO/(s m^2) – is slightly changed. Thus, for the A-2 composite the activity is 0.011 mL CO/(s m^2), while for A-6 and A-7 it is 0.010 and 0.017 mL CO/(s m^2), respectively. The value for the A-2 composite is assessed due to the nonstationary regime of the sample testing at 700 °C, but it does not vary during testing.

Hence, the decrease of Ni content in anode composite materials to 20–15% increases their resistance to coking. This is also confirmed by the TPO study of some samples after testing at 700 °C in methane steam reforming for 270 min (Table 2). The amount of CO_2 evolved due to coke oxidation decreases by six times for the A-6 sample as compared with the A-2 composite.

3.2.4. The effect of the ATLS dopant nature

The catalytic performance of anode materials in SR was shown to be strongly affected by the nature of ATLS dopant. Some results for samples based on Al-doped ATLS are presented in Fig. 5. As well as for the A-2 composite based on Sr-doped ATLS, for the similar A-7 sample a high initial methane conversion accompanied by a low C-product selectivity is observed. However, in contrast to the A-2 sample, the decrease of the methane conversion and increase of the target product selectivity are less pronounced, indicating its higher ability to coking. According to the TPO study, the amount of CO_2 emitted per gram of the A-7 sample after testing at 700 °C for 253 min is close to that of the A-2 sample after testing at 700 °C for 270 min (Table 2). However, according to catalytic experiment, for the A-2 sample the main part of coke is formed during the fist 1.5–2 h of testing, while for the A-7 composite the strong coking occurs during all test duration (Fig. 6).

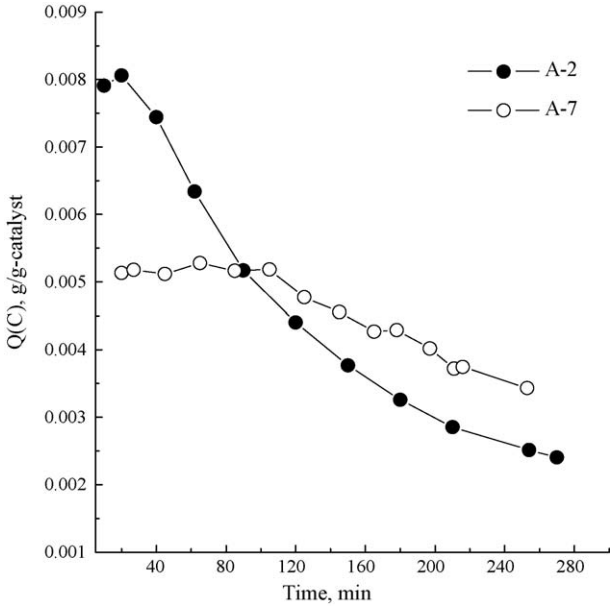

Fig. 6. Time dependence of coke formation according to the catalytic data for anode composite based on apatite-type lanthanum silicates doped by different elements: A-2, 30 wt.% Ni/10 wt.% $La_{0.8}Sr_{0.2}Mn_{0.8}Cr_{0.2}O_3$/60 wt.% $La_9SrSi_6O_{26.5}$; A-7, 30 wt.% Ni/10 wt.% $La_{0.8}Sr_{0.2}Mn_{0.8}Cr_{0.2}O_3$/60 wt.% $La_{9.83}Si_5AlO_{26.25}$.

Moreover, in comparison to samples based on Sr-doped ATLS, the partial Ni substitution by LST in samples based on Al-doped ATLS does not result in improving the catalytic characteristics and suppression of the coke formation. On the contrary, for the A-10 sample, where 50% Ni is substituted, a complete sample deactivation toward methane oxidation due to strong coking is observed already after 2 h of testing (Fig. 5). Such strong coking of the samples is confirmed by the subsequent TPO study (Table 2). Thus, the amount of CO_2 evolved for the A-10 sample after testing at 700 °C for only 120 min does not strongly differ from that of A-2 and A-7 composites and it is significantly higher then the amount of evolved CO_2 for the similar A-6 sample based on Sr-doped ATLS. Besides, the temperature of the CO_2 evolution maximum for samples based on Al-doped ATLS is somewhat higher than that for samples based on Sr-doped ATLS. This can be caused by a different (more dense) nature of a formed coke over these samples.

A strong coking ability of composites based on Al-doped ATLS in comparison with those based on Sr-doped ATLS can be caused by a higher surface acidity of aluminosilicates [22]. Besides, the presence of some Sr-oxide shown by XRD (Fig. 1) can favour the decrease of coke formation in the case of composites based on Sr-doped electrolyte due to blocking step sites on the surface of Ni particles, which are active in carbon formation. A similar effect of K, S or Au are well discussed in the literature [23,24]. However, this issue requires an additional study and the role of apatite surface acidity should be considered as well.

Table 2
Results of the temperature programmed oxidation study of samples after catalytic testing at 700 °C: $Q(CO_2)$, the amount of CO_2 evolved per gram of the sample due to coke oxidation; T_{max}, temperature of maximum CO_2 emission.

Sample	Testing time (min)	$Q(CO_2)$ (mmol/g)	T_{max} (°C)
A-2	270	5.5	578
A-6	270	0.9	604
A-7	253	5.0	600
A-10	120	4.8	622

4. Conclusions

New types of anode materials for multi-fuel IT SOFS based on Al and Sr-doped ATLS were synthesized and their catalytic properties and coke stability were studied. The effects of LSMC complex oxide addition, partial Ni substitution with LST MIEC oxide and ATLS composition on system performances were elucidated. Promotion with LSMC and partial Ni substitution by LST improve stability to coking in the anode composites based on Sr-doped ATLS. Using Al-doped ATLS for anode composites was found to strongly affect the catalytic performance, favouring a strong catalyst coking.

Acknowledgment

This work is supported by EC 6 Framework Program within MATSILC Project.

References

[1] O. Yamamoto, Electrochim. Acta 2423 (2000) 45.
[2] C. Song, Catal. Today 17 (2002) 77.
[3] S.C. Singhal, Solid State Ionics 135 (2000) 305.
[4] E. Kendrick, M.S. Islam, P.R. Slater, J. Mater. Chem. 3104 (2007) 17.
[5] F.M.B. Marques, V.V. Kharton, Ionics 321 (2005) 11.
[6] H. Yoshioka, S. Tanase, Solid State Ionics 176 (2005) 2395.
[7] A. Mineshige, T. Nakao, M. Kobune, T. Yazawa, H. Yoshioka, Solid State Ionics 179 (2008) 1009.
[8] T. Nakao, A. Mineshige, M. Kobune, T. Yazawa, H. Yoshioka, Solid State Ionics 179 (2008) 1567.
[9] H. Yoshioka, Y. Nojiri, S. Tanase, Solid State Ionics (2008), doi:10.1016/j.ssi.2008.07.022.
[10] A. Brisse, A.-L. Sauvet, C. Barthet, S. Beaudet-Savignat, J. Fouletier, Fuel Cells 6 (2006) 59.
[11] S. Beaudet Savignat, M. Chiron, C. Barthet, J. Eur. Ceram. Soc. 27 (2007) 673.
[12] S.P. Jiang, S.H. Chan, J. Mater. Sci. 4405 (2004) 39.
[13] J.E.H. Sansom, P.R. Slater, Annu. Rep. Prog. Chem. 101 (2005) 489.
[14] J. Sfeir, P.A. Buffat, P. Mockli, N. Xanthopoulos, R. Vasquez, H.J. Mathieu, J. Van herle, K.R. Thampi, J. Catal. 202 (2001) 229.
[15] V.A. Sadykov, Yu.V. Borchert, G.M. Alikina, A.I. Lukashevich, N.V. Mezentseva, V.S. Muzykantov, E.M. Moroz, V.A. Rogov, V.I. Zaikovskii, D.A. Zyuzin, N.F. Uvarov, A.V. Ishchenko, V.V. Zyryanov, A. Smirnova, Glass Phys. Chem. 33 (2007) 320.
[16] T. Kharlamova, S. Pavlova, V. Sadykov, T. Krieger, G. Alikina, J. Frade, Chr. Argirusis, Mater. Res. Soc. Symp. Proc. The Hydrogen Economy, San Francisco, CA, March 24–28, vol. 1098E, Warrendale, PA, 2008, paper no. 1098-HH07-02.
[17] Ceramics Science and Technology: Structures, vol. 1, Wiley, John & Sons, Incorporated, 2008, p. 612.
[18] M.D. Gross, J.M. Vohs, R.J. Gorte, J. Mater. Chem. 3071 (2007) 17.
[19] H. Kim, C. Lu, W.L. Worrell, J.M. Vohs, R.J. Gorte, J. Electrochem. Soc. 247 (2002) 149.
[20] J.B. Goodenough, Y.-H. Huang, J. Power Sources 1 (2007) 173.
[21] S. Hui, A. Petric, J. Eur. Ceram. Soc. 22 (2002) 1673.
[22] I.D. Micheikin, Soros Educ. J. 5 (2001) 43.
[23] H.S. Bengaard, J.K. Norskov, J. Sehested, B.S. Clausen, L.P. Nielsen, A.M. Molenbroek, J.R. Rostrup-Nielsen, J. Catal. 209 (2002) 365.
[24] N.M. Galea, D. Knapp, T. Ziegler, J. Catal. 247 (2007) 20.